THE EMC OF ELECTRICAL SYSTEMS – GALVANIC COUPLING

(PART II.)

[*]Irena KOVÁČOVÁ, [*]Ján KAŇUCH, [**]Dobroslav KOVÁČ
[*]Department of Electrical Drives and Mechatronics, Technical University of Košice, Letná 9, 042 00 Košice
[**]Department of Theoretical Electrical Engineering and Electrical Measurement, Park Komenského 3,
042 00 Košice, Slovak Republic.
Tel: +421-55-6022273; Fax: +421-55-6330115
E-mail: Irena.Kovacova@tuke.sk, E-mail: Jan.Kanuch@tuke.sk, E-mail: Dobroslav.Kovac@tuke.sk

SUMMARY

This papers deals with the analysis of the electromagnetic compatibility (EMC) – galvanic coupling problems focused on the area of the power electrical systems. The description of galvanic coupling problem is divided into two separate parts according to the length of common conductors or the working frequency. The first part (PART I.) deals with the galvanic coupling problem of concentrated parameter circuits, such with short common conductors or processed signals with low working frequency. The second one (PART II.) analyzes the same problem for circuits with distributed parameters, such that have long common conductors or processed signals with high working frequency. For detailed problem investigation a mathematical analysis, computer simulation method and verification measuring are used, too.

Keywords: *electromagnetic compatibility, galvanic coupling, common conductors, long lines*

1. INTRODUCTION

The problem of galvanic coupling deals with individual electric equipment or their part's interconnections in such a way, that minimum one or (in some cases as for example feeding net) more common conductors interconnecting these equipments and so mutual influence is generated.

2. SOLUTION FOR THE HIGHER FREQUENCIES AND DISTRIBUTED PARAMETERS

The working frequencies and the lengths of common conductor must be taken always into account. In all cases of the galvanic coupling, the fact that electrical components are not ideal and so they are containing certain parasitic capacitances, inductances and real resistances is valid. Due to higher working frequency of currents flowed by the common conductors, they must be taken as circuits with distributed parameters during the process of predictive result galvanic coupling investigation. If the working frequencies will be lower, then the interconnecting circuits can be taken as circuits with concentrated parameters.

2.1. Two common conductors - theoretical analysis

The mutual interconnection of electric circuits by two common conductors with the length *l* (the length is long or the transferred signal has high frequency) represents the investigation problem of a line with distributed parameters (in the following "long transmission line" or "long line" only). The basic representation of such electric circuit interconnection is drawn in figure Fig. 1.
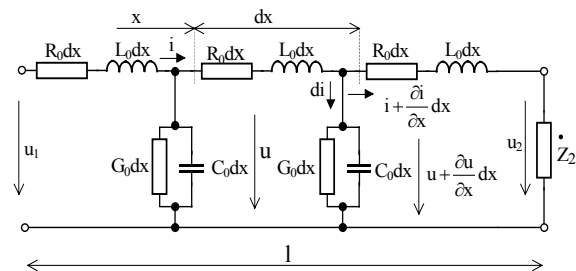

Fig. 1 The spare scheme of long transmission line with distributed parameters

It is known from the electric circuit theory that the time dependence investigation of line voltage or current, at optional line position, leads to the system solution of two partial-differential equations.

$$-\frac{\partial u}{\partial x} = L_0 \frac{\partial i}{\partial t} + R_0 i \tag{1}$$

$$-\frac{\partial i}{\partial x} = G_0 u + C_0 \frac{\partial u}{\partial t} \tag{2}$$

In that case an input voltage and a current of long transmission line it is possible to describe by time harmonic functions in the form,

$$u = U_m \sin(\omega t + \psi_u) \quad \Rightarrow \quad \overset{\bullet}{U} e^{j\omega t} \tag{3}$$

$$i = I_m \sin(\omega t + \psi_i) \quad \Rightarrow \quad \overset{\bullet}{I} e^{j\omega t} \tag{4}$$

the resulting solution of the given equation system, expressed by complex voltage and current phasors, will be given as:

$$\overset{\bullet}{U} = \overset{\bullet}{U_1} ch \overset{\bullet}{\gamma} x - Z_v \overset{\bullet}{I_1} sh \overset{\bullet}{\gamma} x \tag{5}$$

$$\overset{\bullet}{I} = \overset{\bullet}{I_1} ch \overset{\bullet}{\gamma} x - \frac{\overset{\bullet}{U_1}}{\overset{\bullet}{Z_v}} sh \overset{\bullet}{\gamma} x \tag{6}$$

where

$$\dot{\gamma} = \beta + j\alpha = \sqrt{(R_0 + j\omega L_0)(G_0 + j\omega C_0)} \qquad (7)$$

$$\beta = \sqrt{\frac{1}{2}\left[\sqrt{(R_0^2 + \omega^2 L_0^2)(G_0^2 + \omega^2 C_0^2)} + R_0 G_0 - \omega^2 L_0 C_0\right]} \qquad (8)$$

$$\alpha = \sqrt{\frac{1}{2}\left[\sqrt{(R_0^2 + \omega^2 L_0^2)(G_0^2 + \omega^2 C_0^2)} - R_0 G_0 + \omega^2 L_0 C_0\right]} \qquad (9)$$

$$\dot{Z}_v = \sqrt{\frac{(R_0 + j\omega L_0)}{(G_0 + j\omega C_0)}} = Z.e^{j\varphi_v} \qquad (10)$$

In the field of power electronics a non-harmonic unipolar or bipolar signal is utilized many times for indirect converters. To enable a given problem's mathematical analysis, the non-harmonic signal must be described by the system of harmonic functions.

Let the input feeding voltage of a long transmission line with distributed parameters have the time dependence pictured in figure Fig. 2. Its description by harmonic components will be done on the basis of Fourier's series, the coefficients of which is given as:
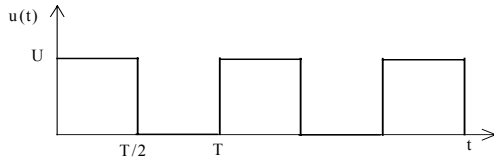

Fig. 2 The non-harmonic feeding voltage of long transmission line

$$a_0 = \frac{1}{T}\int_0^T f(\omega t)dt = \frac{1}{T}\int_0^{T/2} U.dt = \frac{U}{2} \qquad (11)$$

$$a_k = \frac{2}{T}\int_0^T f(\omega t).\cos(k\omega t)dt = \frac{2}{T}\int_0^{T/2} U.\cos(k\omega t)dt = \frac{U}{k\pi}(\sin(k\pi) - 0) = 0 \qquad (12)$$

$$b_k = \frac{2}{T}\int_0^T f(\omega t).\sin(k\omega t)dt = \frac{2}{T}\int_0^{T/2} U.\sin(k\omega t)dt = -\frac{U}{k\pi}(\cos(k\pi) - 1) \qquad (13)$$

The expression of the investigated voltage time dependence will be done by calculated coefficients of Fourier's series and by the next equation.

$$u(t) = \sum_{k=0}^{\infty}(a_k.\cos(k\omega t) + b_k\sin(k\omega t)) \qquad (14)$$

$$u(t) = \frac{U}{2} + \frac{2U}{\pi}\sin(\omega t) + \frac{2U}{3\pi}\sin(3\omega t) + \frac{2U}{5\pi}\sin(5\omega t) + ... =$$
$$= \frac{U}{2} + \sum_{k=0}^{\infty}\frac{2U}{(2k+1)\pi}\sin((2k+1)\omega t) \qquad (15)$$

For a long line galvanic coupling influence investigation, it is necessary to obtain the time dependence of the voltage at the end of the long transmission line. It is possible to calculate the searched voltage on the basis of an equation expressing the time voltage dependence at an optional position of a long transmission line, which is far-away from the beginning of the line about the distance x so, that this length will be replaced by the line length l and the complex current vector $\dot{I}_1$ will be replaced by the relation $\dot{U}_1 / \dot{Z}_{input}$.

$$\dot{U}_2 = \dot{U}_1 ch\ \dot{\gamma} l - \dot{Z}_v \dot{I}_1 sh\ \dot{\gamma} l = \dot{U}_1 ch\ \dot{\gamma} l - \dot{Z}_v \frac{\dot{U}_1}{\dot{Z}_{input}} sh\ \dot{\gamma} l \qquad (16)$$

$$\dot{U}_2 = \dot{U}_1(ch\ \dot{\gamma} l - \frac{\dot{Z}_2 sh\ \dot{\gamma} l + \dot{Z}_v ch\ \dot{\gamma} l}{\dot{Z}_2 ch\ \dot{\gamma} l + \dot{Z}_v sh\ \dot{\gamma} l}.sh\ \dot{\gamma} l) \qquad (17)$$

$$\dot{U}_2 = U_1.e^{j\varphi_U}(\frac{1}{2}(e^{\dot{\gamma} l} + e^{-\dot{\gamma} l}) -$$
$$- \frac{Z_2.e^{j\varphi_{Z2}}.\frac{1}{2}(e^{\dot{\gamma} l} - e^{-\dot{\gamma} l}) + Z_v.e^{j\varphi_{Zv}}.\frac{1}{2}(e^{\dot{\gamma} l} + e^{-\dot{\gamma} l})}{Z_2.e^{j\varphi_{Z2}}.\frac{1}{2}(e^{\dot{\gamma} l} + e^{-\dot{\gamma} l}) + Z_v.e^{j\varphi_{Zv}}.\frac{1}{2}(e^{\dot{\gamma} l} - e^{-\dot{\gamma} l})}.\frac{1}{2}(e^{\dot{\gamma} l} - e^{-\dot{\gamma} l})) \qquad (18)$$

$$\dot{U}_2 = \frac{U_1}{2}.((e^{(\beta l + j(\alpha l + \varphi_U))} + e^{-(\beta l + j(\alpha l - \varphi_U))}) -$$
$$- \frac{a + jb}{c + jd}.(e^{(\beta l + j(\alpha l + \varphi_U))} - e^{-(\beta l + j(\alpha l - \varphi_U))})) \qquad (19)$$

where the expressions $\dot{Z}_{input}$, a, b, c, d are calculated on the basis of following equations:

$$\dot{Z}_{input} = \frac{\dot{Z}_2 ch\ \dot{\gamma} l + \dot{Z}_v sh\ \dot{\gamma} l}{\dfrac{\dot{Z}_2 sh\ \dot{\gamma} l}{\dot{Z}_v} + ch\ \dot{\gamma} l} \qquad (20)$$

$$a = Z_2.e^{\beta l}.\cos(\alpha l + \varphi_{Z2}) - Z_2.e^{-\beta l}.\cos(\varphi_{Z2} - \alpha l) +$$
$$+ Z_v.e^{\beta l}.\cos(\alpha l + \varphi_{Zv}) + Z_v.e^{-\beta l}.\cos(\varphi_{Zv} - \alpha l) \qquad (21)$$

$$b = Z_2.e^{\beta l}.\sin(\alpha l + \varphi_{Z2}) - Z_2.e^{-\beta l}.\sin(\varphi_{Z2} - \alpha l) +$$
$$+ Z_v.e^{\beta l}.\sin(\alpha l + \varphi_{Zv}) + Z_v.e^{-\beta l}.\sin(\varphi_{Zv} - \alpha l) \qquad (22)$$

$$c = Z_2.e^{\beta l}.\cos(\alpha l + \varphi_{Z2}) + Z_2.e^{-\beta l}.\cos(\varphi_{Z2} - \alpha l) +$$
$$+ Z_v.e^{\beta l}.\cos(\alpha l + \varphi_{Zv}) - Z_v.e^{-\beta l}.\cos(\varphi_{Zv} - \alpha l) \qquad (23)$$

$$d = Z_2.e^{\beta l}.\sin(\alpha l + \varphi_{Z2}) + Z_2.e^{-\beta l}.\sin(\varphi_{Z2} - \alpha l) +$$
$$+ Z_v.e^{\beta l}.\sin(\alpha l + \varphi_{Zv}) - Z_v.e^{-\beta l}.\sin(\varphi_{Zv} - \alpha l) \qquad (24)$$

When substituting all known parameters, the relation modification and the imaginary part of the resulting complex form will be taken into account, because only this corresponds to the input voltage sinusoidal course, so we can obtain the final formula for the searched voltage at the end of the line.

$$u_2(t) = \frac{R_2 U}{2(R_0.R_2.G_0 + R_0 + R_2)} + \sum_{k=0}^{\infty}\frac{U}{(2k+1)\pi}.(e^{\beta l}.\sin((2k+1)\omega t +$$
$$+ \varphi_U + \alpha l) + e^{-\beta l}.\sin((2k+1)\omega t + \varphi_U - \alpha l) - \frac{\sqrt{a^2 + b^2}}{\sqrt{c^2 + d^2}}.e^{\beta l}.$$
$$.\sin((2k+1)\omega t + \varphi_U + \alpha l + arctg\frac{b}{a} - arctg\frac{d}{c}) + \frac{\sqrt{a^2 + b^2}}{\sqrt{c^2 + d^2}}.e^{-\beta l}.$$
$$.\sin((2k+1)\omega t + \varphi_U - \alpha l + arctg\frac{b}{a} - arctg\frac{d}{c})) \qquad (25)$$

The graphical presentation of the searched course and its comparison with the input course can be realized for example by the Excel program. For the derived equation's practical verification purpose, the interconnection of one quadrant impulse conver-ter and resistive-inductive load $R_2 = 10\ \Omega$, $L_2 = 1$ mH by CYSY 4x1,5 mm^2 cable, with the length 15m and parameters $R_0 = 0{,}047\ \Omega$/m, $L_0 = 343$ nH/m, $G_0 = 33{,}3\ \mu$S/m, $C_0 = 118$ pF/m, is chosen. The converter's switching frequency is 40 kHz and the supply voltage has the value $U = 70$ V. The comparative results for the input and output voltages are shown in figures Fig. 3 and Fig. 4.
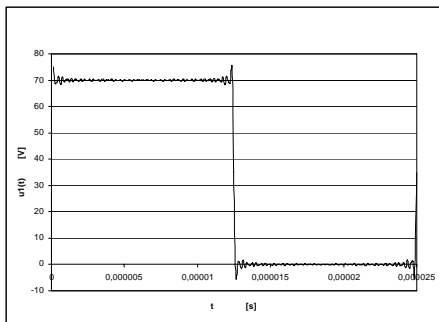
Fig. 3 The voltage at the start of line
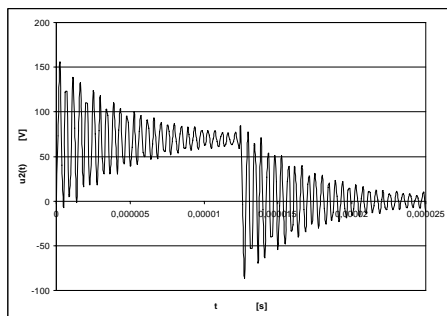
Fig. 4 The voltage at the end of line

By the comparison of both pictures, it is possible to state that due to long transmission line properties, the additional damped oscillations are generated at the moment of transient states. The amplitude of these oscillations can reach the amplitude of the input feeding voltage. From the analysis, it is also evident, that if the long transmission line or load would have other parameters, standing undulating can be generated. It is also possible to discover that if the load is adapted, then no oscillation would be done. It is the case, when the back reflected wave is not starting up, and so the mutual influence of galvanic coupling is not coming into existence, too.

2.2. Two common conductors – simulation and measuring

The PSPICE program will do the verification simulations. All the line-distributed parameters can be replaced by concentrated ones for the given long line position (in our case it is end of long line). These parameters are calculated for the given long

transmission line length. The equivalent scheme for the PSPICE program simulation is displayed in figure Fig. 5. The resulting curves, obtained by simulation, are in figure Fig. 6.
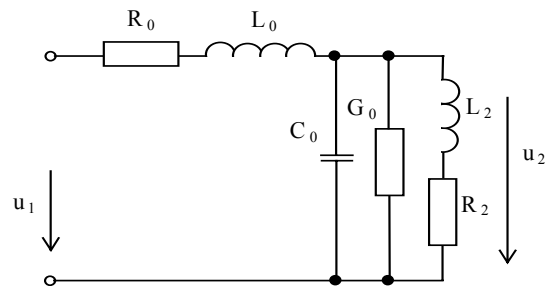

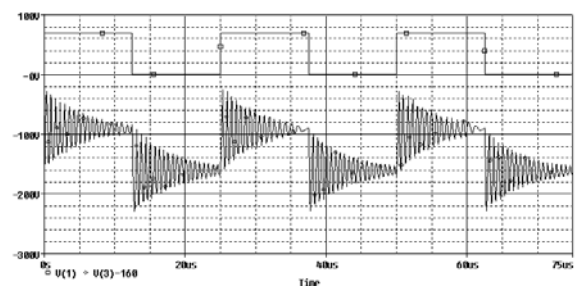**Fig. 5** The equivalent scheme for PSPICE program simulation

Fig. 6 The simulation results

The measured curves of the comparable voltages are displayed in the following two figures Fig. 7 and Fig. 8.
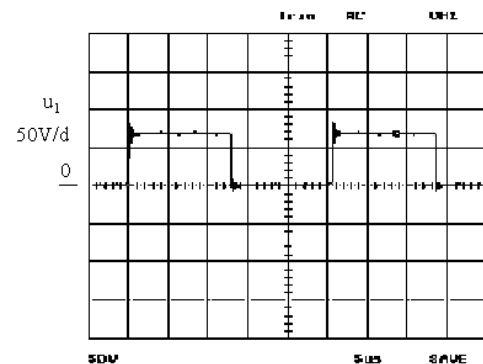

Fig. 7 The voltage at the beginning of the long line
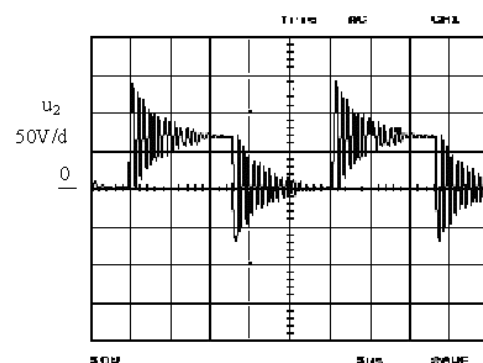

Fig. 8 The voltage at the end of the long line

By the comparison of all the results obtained by the three methods, it is possible to state, that the derived equations are correct, and should be utilized for a predictive investigation of galvanic coupling influence, caused by the existence of two common conductors of the long transmission line.

2.3. One common conductor - theoretical analysis

The electric circuits interconnection realized by one common conductor with the distributed parameters, is a special case, where more electric circuits are utilizing one common conductor, which is either long or serves for high frequency signal conduction, as it is pictured in figure Fig. 9.
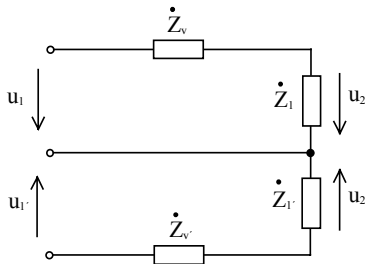
Fig. 9 The circuit interconnection by one common conductor - higher frequencies

The problem analysis will be done for the case of two electric circuits interconnection, the scheme of which is shown in figure Fig. 10. Let the upper circuit be supplied by a DC voltage source with the value $U_1 = 5$ V. As interface conductor the same cable as in the previous case was used, it means a CYSY 4x1,5 mm^2 with the length 15m and with parameters $R_{0'} = 0,047$ Ω/m, $L_{0'} = 343$ nH/m, $G_{0'} = 33,3$ μS/m, $C_{0'} = 118$ pF/m.
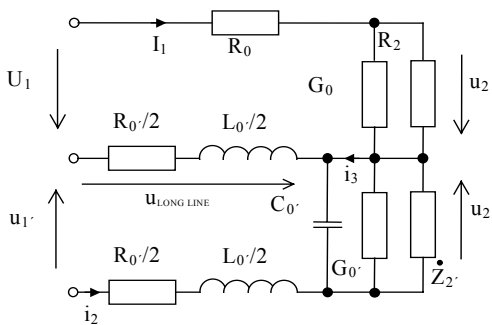

Fig. 10 The scheme of investigated circuit connection

The upper circuit has no signal change. The output voltage u_2 should be reflecting only the voltage drops caused by long line longitudinal resistance and a vertical drop-in. Let the lower circuit be supplied by the same periodical impulse signal $u_{1'}$ as in the case of the previous analysis. It is possible to state the mutual circuit galvanic coupling influence by finding the upper circuit real voltage u_2 course. According to the 2nd Kirchoff's law, we can write the equation for the investigated circuit:

$$u_2 = U_1 - u_{1'} + u_{2'} - R_0.I_1 = U_1 - u_{1'} + u_{2'} - R_0.\frac{U_1}{\frac{R_2.G_0}{R_2 + G_0} + R_0} \quad (26)$$

The analytical form for the voltages $u_{1'}$ and $u_{2'}$ the description can be obtained, from the previous analysis, as equations for input and output voltages of long transmission line. By the substitution of these voltages, the searched relation for time dependence of the voltage u_2 is possible to receive. Any accessible Excel program will do the graphical interpretation of the resulting solution again, figures Fig. 11 up to Fig. 14.
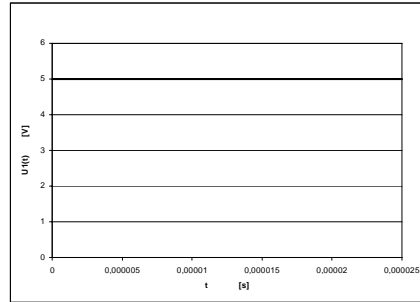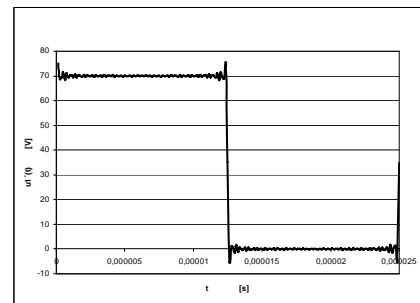

Fig. 11 The input voltage U_1

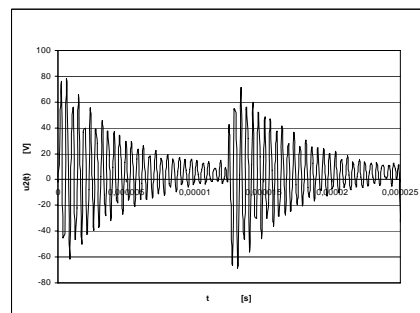**Fig. 12** The input voltage $u_{1'}$
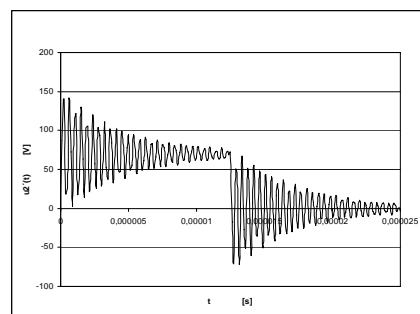

Fig. 13 The output voltage u_2

Fig. 14 The output voltage $u_{2'}$

2.4. One common conductor – simulation and measuring

Equally, as in the previous case a multiple verification of correctness can be done by the PSPICE program simulation and by practical measurement.
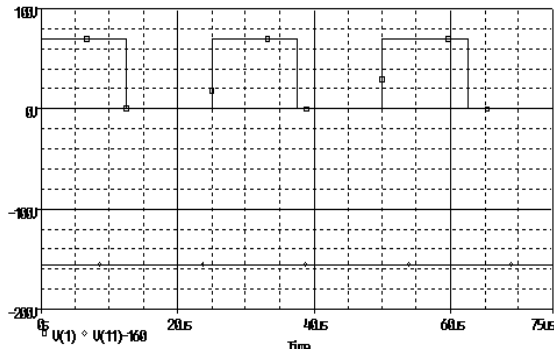

Fig. 15 The input voltages $u_{1'}$ and U_1 obtained by simulation in the PSPICE program
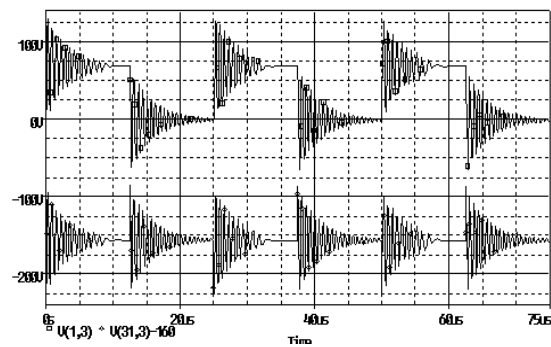

Fig. 16 The input voltages $u_{2'}$ and u_2 obtained by simulation in the PSPICE program

The coincidence of the obtained results is evident. Small differences concerning the input and output voltage oscillation damping are given by the fact, that for the input and output voltages the infinite Fourier's series were replaced by only the first 40 components in the Excel program. The measured courses of the voltages are pictured in next figures Fig. 17 up to Fig. 20.
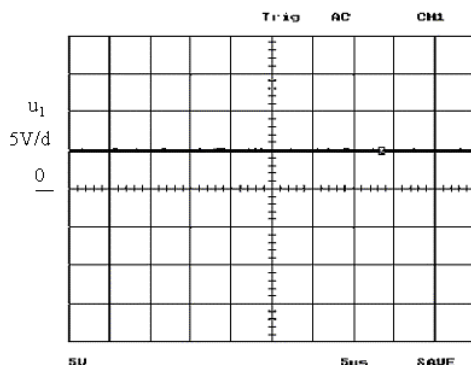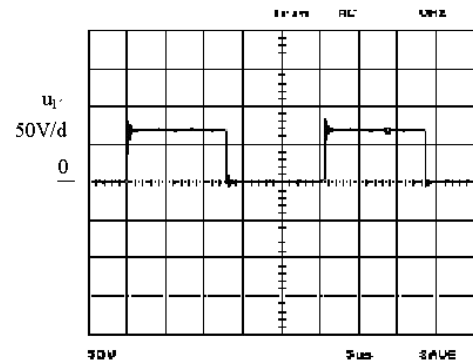

Fig. 17 The measured input voltage u_1

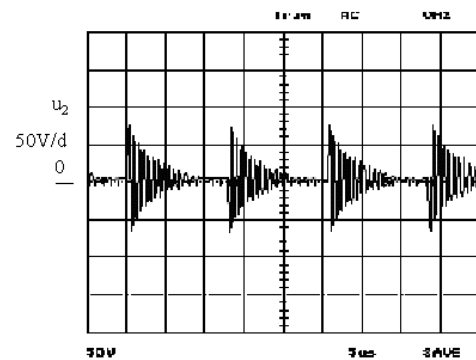**Fig. 18** The measured input voltage $u_{1'}$

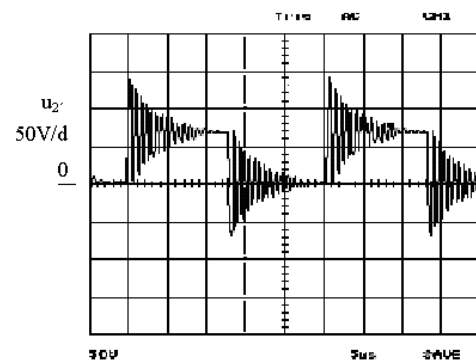**Fig. 19** The measured output voltage u_2

Fig. 20 The measured output voltage $u_{2'}$

2.5. Several common conductors - theoretical analysis

Very often a symmetrical three-phase load is connected to the inverter impulse output, with the frequency of few tenths of kHz, by the cable with the length within the range 3 up to 20 m during the practical use of power semiconductor converters. This case represents the interconnection of two circuits, by a long line with the distributed parameters in the three phases connection, such, which is shown in figure Fig. 21.

Let the galvanic coupling investigation of such circuit topology be done by a temporal dependence calculation of the voltages $u_{12'}$, $u_{23'}$ and $u_{31'}$ at the end position of a long transmission line. The input long line voltages are graphically depicted in figure Fig. 22.
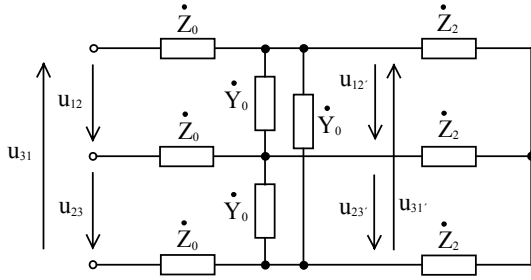
Fig. 21 The circuit interconnection by several common conductors and higher frequencies
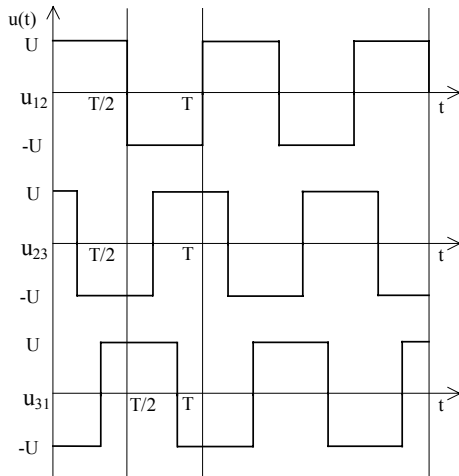

Fig. 22 The input voltages u_{12} , u_{23} and u_{31}

The amplitudes of the input voltages are U = 400 V. The same interconnecting cable was used as in the previous case with the parameters: CYSY 4x1,5 mm^2 ,with the length 15m, R_0 = 0,047 Ω/m, L_0 = 343 nH/m, G_0 = 33,3 μS/m, C_0 = 118 pF/m. The load is symmetrical, resistive-inductive with parameters R_2 = 10 Ω, L_2 = 1 mH. For the calculation of the output voltages $u_{12'}$, $u_{23'}$ and $u_{31'}$ can be used the relations derived in previous analyses, but it is necessary to express the non-harmonic input feeding voltages of the long transmission line by a harmonic functions. The Fourier's series will be used again.

$$a_0 = \frac{1}{T} \int_0^{T/2} U\,.dt + \frac{1}{T} \int_{T/2}^{T} -U\,.dt = 0 \qquad (27)$$

$$a_k = \frac{2}{T} \int_0^{T/2} U.\cos(k\omega t)dt + \frac{2}{T} \int_{T/2}^{T} -U.\cos(k\omega t)dt = \frac{U}{k\pi}(((\sin(k\pi) - \sin(0)) - (\sin(k2\pi) - \sin(k\pi))) = 0 \qquad (28)$$

$$b_k = \frac{2}{T} \int_0^{T/2} U.\sin(k\omega t)dt + \frac{2}{T} \int_{T/2}^{T} -U.\sin(k\omega t)dt = -\frac{U}{k\pi}((\cos(k\pi) - 1) - (\cos(k2\pi) - \cos(k\pi))) = \frac{4U}{(2k+1)\pi} \qquad (29)$$

$$u_{12}(t) = \frac{4U}{\pi}\sin(\omega t) + \frac{4U}{3\pi}\sin(3\omega t) + \frac{4U}{5\pi}\sin(5\omega t) + ... = \sum_{k=0}^{\infty} \frac{4U}{(2k+1)\pi}\sin((2k+1)\omega t) \qquad (30)$$

The two other voltages are possible to express by the sentence about translation.

$$u_{23}(t) = \frac{4U}{\pi}\sin(\omega(t-\frac{T}{3})) + \frac{4U}{3\pi}\sin(3\omega(t-\frac{T}{3})) + \frac{4U}{5\pi}\sin(5\omega(t-\frac{T}{3})) + ... = \sum_{k=0}^{\infty} \frac{4U}{(2k+1)\pi}\sin((2k+1)\omega(t-\frac{T}{3})) \qquad (31)$$

$$u_{31}(t) = \frac{4U}{\pi}\sin(\omega(t-\frac{2T}{3})) + \frac{4U}{3\pi}\sin(3\omega(t-\frac{2T}{3})) + \frac{4U}{5\pi}\sin(5\omega(t-\frac{2T}{3})) + ... = \sum_{k=0}^{\infty} \frac{4U}{(2k+1)\pi}\sin((2k+1)\omega(t-\frac{2T}{3})) \qquad (32)$$

If the calculated relations for the input voltages are substituted by the derived equation (19), which describes the temporal dependence of the voltage at the end of the long line and only the imaginary part of the complex solution will be taken into account, because only this part corresponds to the sinusoidal input voltage, thus we can obtain the relations (33) up to (35).

During the calculation process, the load impedance value recalculation from star to triangle could not be forgotten, because the temporal curves of interline voltages are searched. The Excel program utilized for the first 40 components of Fourier's series will again do the graphical representation of the obtained results. The respective curves are drawn in figures Fig. 23 up to Fig. 28.
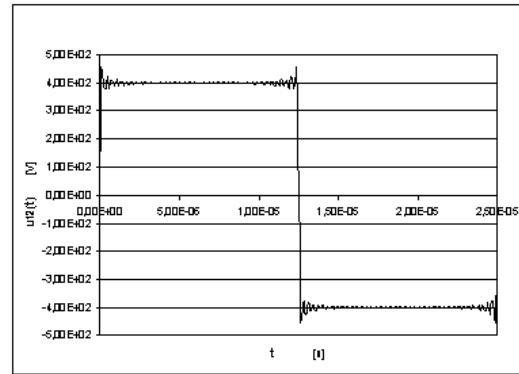

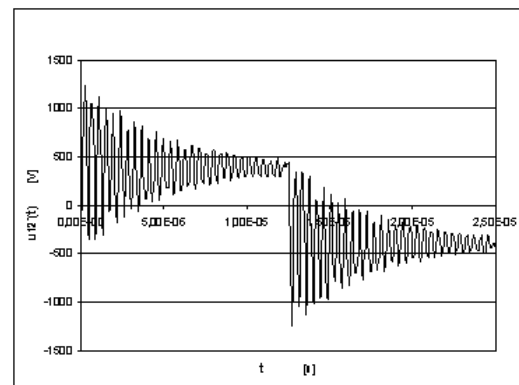**Fig. 23** The input voltage u_{12} synthesis

Fig. 24 The output voltage $u_{12'}$

$$u_{12'}(t) = \sum_{k=0}^{\infty} \frac{2U}{(2k+1)\pi} \cdot (e^{\beta l} \cdot \sin((2k+1)\omega t + \varphi_U + \alpha l) + e^{-\beta l} \cdot \sin((2k+1)\omega t + \varphi_U - \alpha l) - \frac{\sqrt{a^2+b^2}}{\sqrt{c^2+d^2}} \cdot e^{\beta l} \cdot$$

$$\cdot \sin((2k+1)\omega t + \varphi_U + \alpha l + arctg\frac{b}{a} - arctg\frac{d}{c}) + \frac{\sqrt{a^2+b^2}}{\sqrt{c^2+d^2}} \cdot e^{-\beta l} \cdot \sin((2k+1)\omega t + \varphi_U - \alpha l + arctg\frac{b}{a} - arctg\frac{d}{c}))$$

(33)

$$u_{23'}(t) = \sum_{k=0}^{\infty} \frac{2U}{(2k+1)\pi} \cdot (e^{\beta l} \cdot \sin((2k+1)\omega(t-\frac{T}{3}) + \varphi_U + \alpha l) + e^{-\beta l} \cdot \sin((2k+1)\omega(t-\frac{T}{3}) + \varphi_U - \alpha l) - \frac{\sqrt{a^2+b^2}}{\sqrt{c^2+d^2}} \cdot e^{\beta l} \cdot$$

$$\cdot \sin((2k+1)\omega(t-\frac{T}{3}) + \varphi_U + \alpha l + arctg\frac{b}{a} - arctg\frac{d}{c}) + \frac{\sqrt{a^2+b^2}}{\sqrt{c^2+d^2}} \cdot e^{-\beta l} \cdot \sin((2k+1)\omega(t-\frac{T}{3}) + \varphi_U - \alpha l + arctg\frac{b}{a} - arctg\frac{d}{c}))$$

(34)

$$u_{31'}(t) = \sum_{k=0}^{\infty} \frac{2U}{(2k+1)\pi} \cdot (e^{\beta l} \cdot \sin((2k+1)\omega(t-\frac{2T}{3}) + \varphi_U + \alpha l) + e^{-\beta l} \cdot \sin((2k+1)\omega(t-\frac{2T}{3}) + \varphi_U - \alpha l) - \frac{\sqrt{a^2+b^2}}{\sqrt{c^2+d^2}} \cdot e^{\beta l} \cdot$$

$$\cdot \sin((2k+1)\omega(t-\frac{2T}{3}) + \varphi_U + \alpha l + arctg\frac{b}{a} - arctg\frac{d}{c}) + \frac{\sqrt{a^2+b^2}}{\sqrt{c^2+d^2}} \cdot e^{-\beta l} \cdot \sin((2k+1)\omega(t-\frac{2T}{3}) + \varphi_U - \alpha l + arctg\frac{b}{a} - arctg\frac{d}{c}))$$
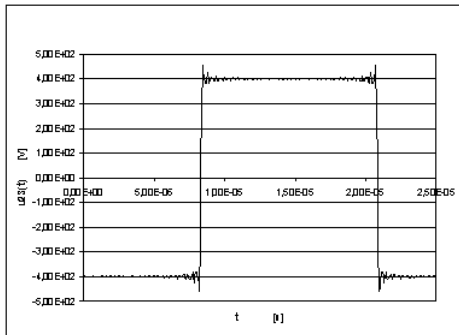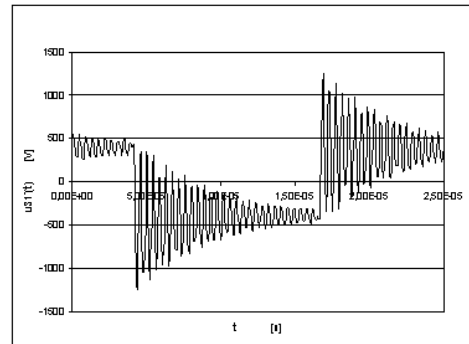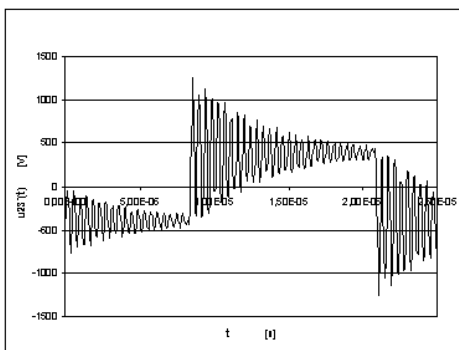
(35)

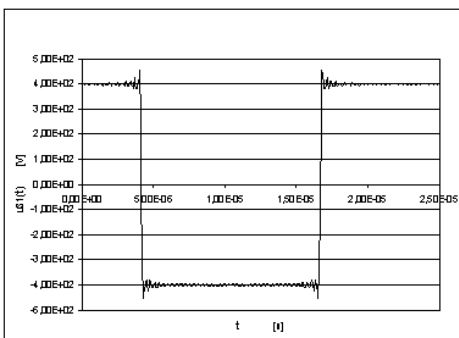**Fig. 25** The input voltage u_{23} synthesis

Fig. 28 The output voltage $u_{31'}$

Fig. 26 The output voltage $u_{23'}$

The following two figures show the sum of all three input and output interline voltages. From the courses, it is evident, that during such a choice of feeding signal shape, the non-harmonic supply system, containing the expressive amount of 3rd harmonic voltage and its multiples, is generated. In the case of four-conductor circuit interconnection, the loop current, flowing via a neutral wire, is created by the resulting potential of the source node, which is in contradiction to the standard requirements.
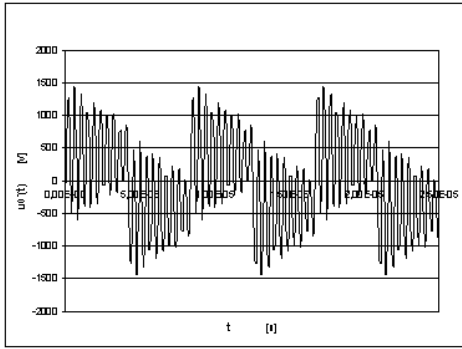

Fig. 27 The input voltage u_{31} synthesis
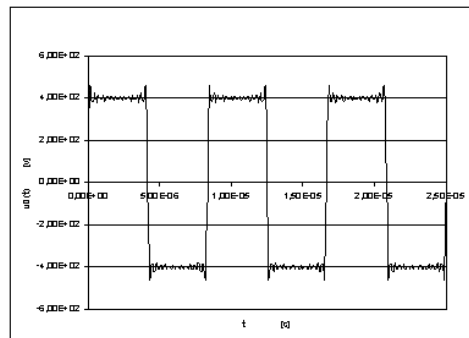
Fig. 29 The potential of the source node

Fig. 30 The potential of the load node

2.6. Several common conductors - simulation and measuring

For the subsidiary verification simulations, the Excel program can be utilized again. The long transmission line, with the distributed parameters will be replaced by a concentrate parameters corresponding to its length. The simulation results are displayed in the following two figures Fig. 31 and Fig. 32.
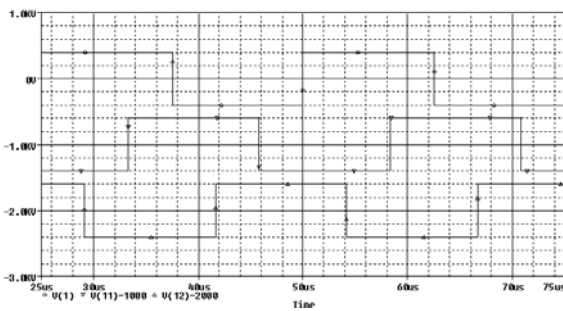
Fig. 31 The input non-harmonic voltages of the three-phase load system obtained by simulation
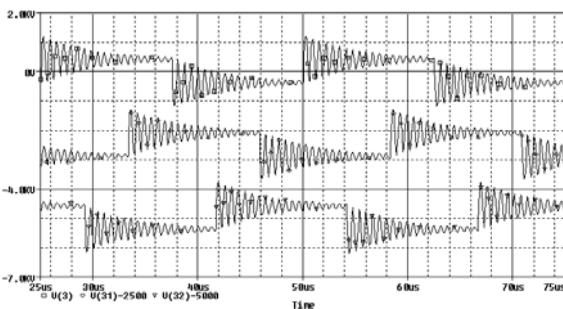
Fig. 32 The output voltages of the three-phase load system obtained by simulation

The coincidence between the courses obtained by analytical calculation and by the simulation method is evident. So we can just suppose, that the derived relations are correct. The verified measurement results are shown in the following figures Fig. 33 up to Fig. 38.

Fig. 33 The input voltage u_{12}

Fig. 34 The output voltage $u_{12'}$

Fig. 35 The input voltage u_{23}

Fig. 36 The output voltage $u_{23'}$

Fig. 37 The input voltage u_{31}

Fig. 38 The output voltage $u_{31'}$

2.7. The circuit interconnection by two or several common conductors - theoretical analysis

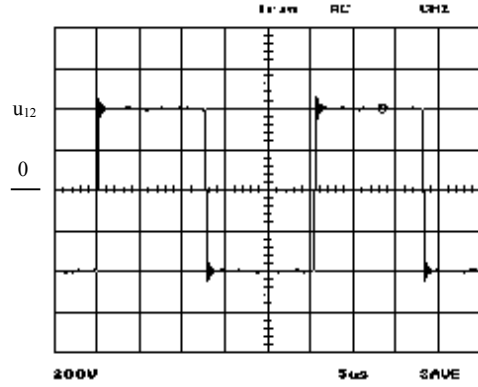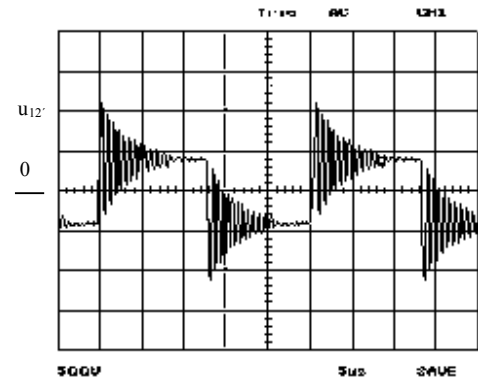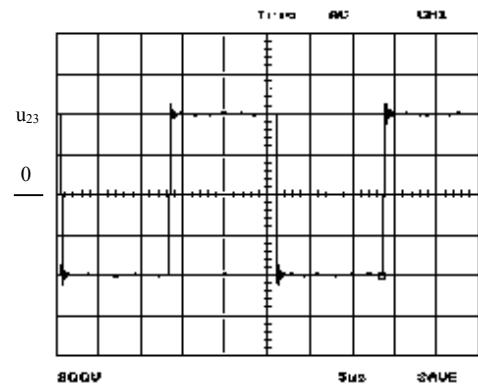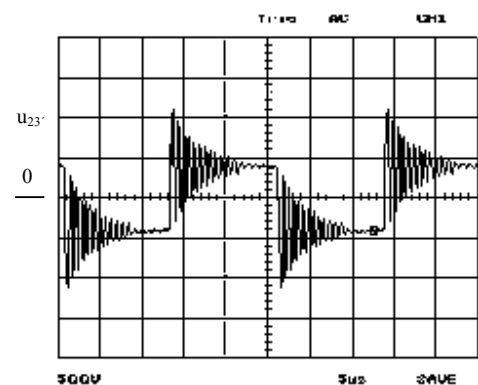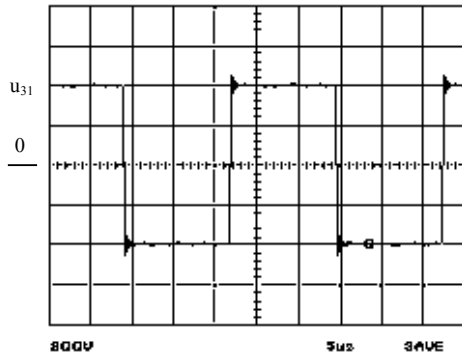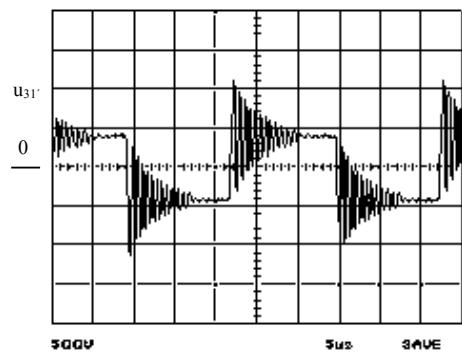For the purpose of the EMC quality arbitration in the case of the existence of galvanic coupling between the electrical equipment and AC feeding net, the coefficients known as selected harmonic distortion factor k_d and total harmonic factor k_s (or THF) are usually used, which are defining the rate of the equipment back influence on the feeding net.

The selected harmonic distortion factor k_d is defined as the ratio of the RMS value (root mean square value) of selected harmonic component and the RMS value of the total non-harmonic course. For the voltage and the 1st harmonic component it is defined as:

$$k_d = \frac{U_1}{U} \tag{36}$$

For the harmonic course $k_d = 1$. The industrial net voltage will be supposed as harmonic, if the difference of two optional samples of 1st harmonic component course and the total voltage course will be smaller than 5 % in the same sampling time.

The total harmonic factor k_s is defined as the quotient of the RMS value of higher harmonic series and non-harmonic RMS value. For the voltage it is given as:

$$k_s = \sqrt{\frac{U_2^2 + U_3^2 + ... + U_k^2}{U_1^2 + U_2^2 + U_3^2 + ... + U_k^2}} \tag{37}$$

For harmonic voltages the relation $k_s = 0$ is valid.

The back influences of individual equipment on the feeding net cause the deformations of the net harmonic voltages and currents, and also the change of the electrical energy quality, for the rest consumers connected to the feeding net. For the non-harmonic periodical curves described in the Fourier's series, it is utilized again. The investigated course is then possible to express by the equation (14), where the individual coefficients are defined by equations (11) up to (13). The RMS value of non-harmonic current or voltage can be stated by the Fourier's series and by the known relation:

$$I = \sqrt{I_0^2 + I_1^2 + I_2^2 + ... + I_k^2} \tag{38}$$

$$U = \sqrt{U_0^2 + U_1^2 + U_2^2 + ... + U_k^2} \tag{39}$$

Beside the above-mentioned factors the stating of the deformation power value is utilized too, mainly for the cases, where the non-harmonic currents or voltages exist and where it is necessary to state the quality of the electric energy. The active power is defined as the average value of the instantaneous power, during the time of one period.

$$P = \frac{1}{T} \int_0^T u\, i\, dt \tag{40}$$

After the substitution of the non-harmonic voltage and current by the Fourier's series, the next equation will be obtained:

$$P = \frac{1}{T} \int_0^T \left[\sum_{k=0}^{\infty} U_{mk} \sin(k\omega t + \psi_{uk}) \sum_{k=0}^{\infty} I_{mk} \sin(k\omega t + \psi_{ik}) \right] dt \tag{41}$$

Due to the fact, that the integral, from the voltage and the current multiplication, results for different harmonics will be equal to zero, so only the same voltage and the vcurrent harmonics can be taken into account.

$$P = \frac{1}{T} \int_0^T \left[\sum_{k=0}^{\infty} U_{mk} I_{mk} \sin(k\omega t + \psi_{uk}) \sin(k\omega t + \psi_{ik}) \right] dt \tag{42}$$

After integration, the active power will be given as:

$$P = U_0 I_0 + \sum_{k=1}^{\infty} \frac{U_{mk} I_{mk}}{2} \cos \varphi_k \tag{43}$$

where $\varphi_k = \psi_{ik} - \psi_{uk.}$ If the expressions for the current and the voltage RMS values will be substituted to the last equation describing the active power, so the active power of non-harmonic periodical current will be possible to express also by the next relation.

$$P = \sum_{k=0}^{\infty} U_k I_k \cos \varphi_k = U_0 I_0 + U_1 I_1 \cos \varphi_1 + U_2 I_2 \cos \varphi_2 + ... \tag{44}$$

By this relation (44) it can be found out, that the active power of non-harmonic current is equal to the sum of the active powers of the individual harmonics, including DC, too. Based on the analogy

with the harmonic power theory the reactive power of non-harmonic voltage and current can be stated.

$$Q = \sum_{k=1}^{\infty} U_k I_k \sin \varphi_k = U_1 I_1 \sin \varphi_1 + U_2 I_2 \sin \varphi_2 + ... \qquad (45)$$

The apparent power of the non-harmonic periodical current is defined as the multiplication of RMS value of non-harmonic voltage and the RMS value of non-harmonic current. The next relation does its exact definition.

$$S = UI = \sqrt{\sum_{k=0}^{\infty} U_k^2} \sqrt{\sum_{k=0}^{\infty} I_k^2} = \sqrt{\sum_{k=0}^{\infty} U_k^2 \sum_{k=0}^{\infty} I_k^2} \qquad (46)$$

The power factor is defined as the active and apparent powers ratio.

$$\lambda = \cos \varphi_{ekv} = \frac{P}{S} = \frac{\sum_{k=0}^{\infty} U_k I_k \cos \varphi_k}{\sqrt{\sum_{k=0}^{\infty} U_k^2 \sum_{k=0}^{\infty} I_k^2}} \qquad (47)$$

However, the fact that angle φ_{ekv} does not represent the angle shift between current and voltage, must be kept in mind. In the optional steady state, it is valid, that $S^2 \geq P^2 + Q^2$. The relation can express this inequality also as equation:

$$S^2 = P^2 + Q^2 + P_d^2 \qquad (48)$$

where P_d is the distortion power.

2.8. Two or several common conductors - simulation and measuring

One phase bridge rectifier with resistive inductive load and output filtering capacitance C_F is very often utilized in practice. For all that its feeding net back influence will be investigated.
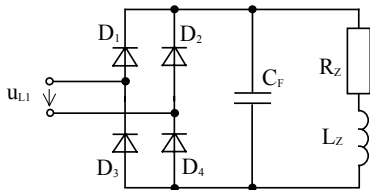
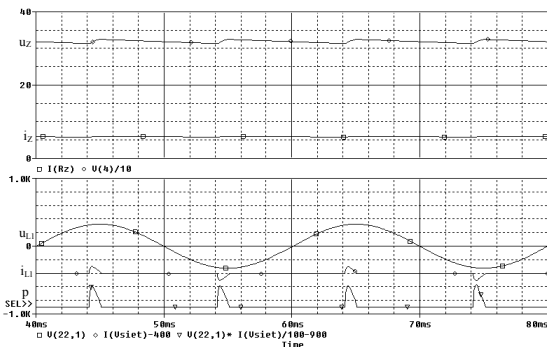**Fig. 39** The investigated circuit scheme

Fig. 40 The input and output voltage and current curves, obtained by simulation in the PSPICE program

The examined circuit scheme is pictured in figure Fig. 39, where $U_{L1} = 230$ V, $R_Z = 53,8$ Ω, $L_Z = 1857,4$ µH, $C_F = 4,7$ mF, $f = 50$ Hz.

The input and output voltage and current curves, obtained by simulation in the PSPICE program, are displayed in figure Fig. 40. The net current non-harmonic shape of course and also due to power's non-harmonic shape of course is evident.

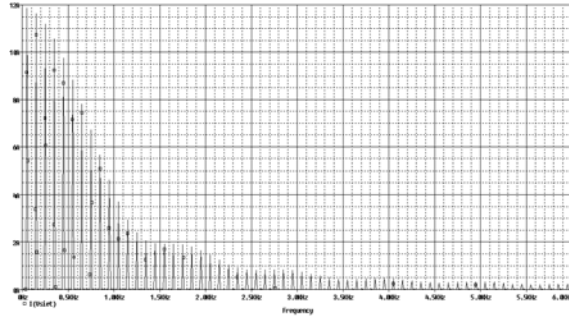The individual harmonics contents in phase net current is introduced in the following figure Fig. 41.

Fig. 41 The phase net current frequency spectrum

The RMS value of the non-harmonic phase current is possible to find out from the next figure Fig. 42. The pictured course was obtained by the use of the PSPICE program's mathematical function.
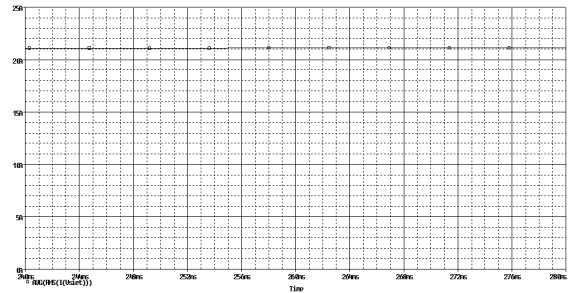
Fig. 42 The RMS value of non-harmonic phase current

The phase angle shift stating for the individual harmonic currents and voltages can be done by the output PSPICE file. If the main PSPICE simulation file contains the command for Fourier analysis performing, the searched values will be generated as it is shown in table Tab. 1.

The first harmonic distortion factor of the voltage and current can be calculated now by the obtained values of shift angles.

$$k_{dU} = \frac{U_1}{U} = \frac{230}{230} = 1 \qquad (49)$$

$$k_{dI} = \frac{I_1}{I} = \frac{11,79}{21,38} = 0,5514 \qquad (50)$$

Similarly, it is possible to express the total harmonic factor of the voltage and current.

$$k_{sU} = \sqrt{\frac{U_2^2 + U_3^2 + ... + U_n^2}{U_1^2 + U_2^2 + U_3^2 + ... + U_n^2}} = \sqrt{\frac{0}{52900}} = 0 \qquad (51)$$

Tab. 1

FOURIER COMPONENTS OF TRANSIENT RESPONSE I(Vnet)					
DC COMPONENT = 2.161637E-04					
HARMONIC NO	FREQUENCY (HZ)	FOURIER COMPONENT	NORMALIZED COMPONENT	PHASE (DEG)	NORMALIZED PHASE (DEG)
1	5.000E+01	1.179E+01	1.000E+00	8.428E+00	0.000E+00
2	1.000E+02	4.737E-02	4.018E-03	-5.258E+01	-6.101E+01
3	1.500E+02	1.156E+01	9.805E-01	-1.547E+02	-1.631E+02
4	2.000E+02	5.725E-02	4.857E-03	1.577E+02	1.492E+02
5	2.500E+02	1.112E+01	9.429E-01	4.230E+01	3.387E+01
6	3.000E+02	6.871E-02	5.828E-03	1.349E+00	-7.078E+00
7	3.500E+02	1.048E+01	8.887E-01	-1.205E+02	-1.290E+02
8	4.000E+02	7.887E-02	6.690E-03	-1.589E+02	-1.673E+02
9	4.500E+02	9.669E+00	8.202E-01	7.691E+01	6.848E+01

$$k_{sI} = \sqrt{\frac{I_2^2 + I_3^2 + \dots + I_n^2}{I_1^2 + I_2^2 + I_3^2 + \dots + I_n^2}} = \sqrt{\frac{318,1003}{457,1044}} = 0,8342 \quad (52)$$

The total active power taken from the net is:

$$P = U_0 I_0 + \sum_{k=1}^{\infty} \frac{U_{mk} I_{mk}}{2} \cos\varphi_k = U_1.I_1.\cos\varphi_1 = 230.11,79.$$
$$.\cos(8,428^o) = 2682,41 \, \text{W} \qquad (53)$$

The amount of reactive power is:

$$Q = \sum_{k=1}^{\infty} U_k I_k \sin\varphi_k = U_1 I_1 \sin\varphi_1 =$$
$$= 230.11,79.\sin(8,428^o) = 397,44 \, \text{VAr} \qquad (54)$$

The quantity of the apparent power is:

$$S = UI = 230.21,38 = 4917,4 \, \text{VA} \qquad (55)$$

The deformation power can be calculated on the basis of the previous relation.

$$P_d = \sqrt{S^2 - P^2 - Q^2} = \sqrt{(4917,4)^2 - (2682,41)^2 - (397,44)^2} =$$
$$= 4102,13 \, \text{VAd} \qquad (56)$$

For the back net influence intensity comparison of the individual rectifier types, the industrial three-phase feeding net is discussed in the following. Its connection is shown in figure Fig. 43, where $U_{12} = U_{23} = U_{31} = 400$ V, $R_Z = 53,8$ Ω, $L_Z = 1857,4$ uH, $C_F = 4,7$ mF, $f = 50$ Hz. The courses of the input and output voltages and currents, obtained by the PSPICE program simulation, are displayed in figure Fig. 44.

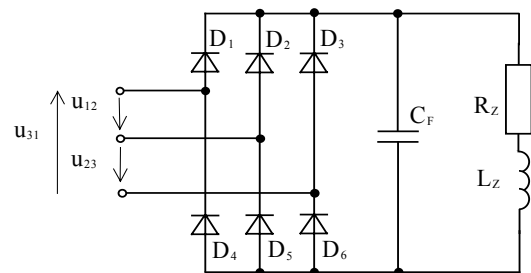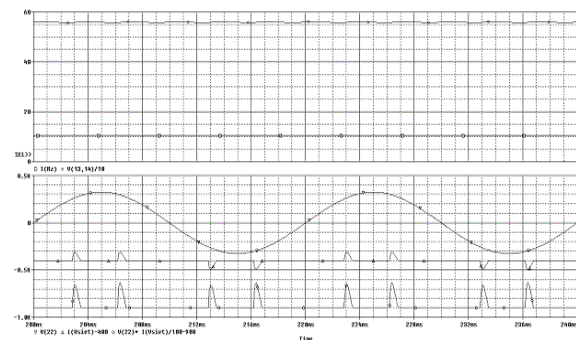**Fig. 43** The investigated circuit connection

Fig. 44 The courses of the input and output voltages and currents, obtained by the PSPICE program simulation

The RMS value of the phase rectifier current is pictured in figure Fig. 45 and the frequency spectrum is displayed in figure Fig. 46. The Fourier's series coefficients are listed in table Tab. 2.

Tab. 2

| FOURIER COMPONENTS OF TRANSIENT RESPONSE I(Vnet)					
DC COMPONENT = -2.449823E-04					
HARMONIC NO	FREQUENCY (HZ)	FOURIER COMPONENT	NORMALIZED COMPONENT	PHASE (DEG)	NORMALIZED PHASE (DEG)
1	5.000E+01	1.203E+01	1.000E+00	3.965E+00	0.000E+00
2	1.000E+02	3.005E-02	2.497E-03	1.337E+02	1.297E+02
3	1.500E+02	3.939E-02	3.273E-03	9.734E+01	9.338E+01
4	2.000E+02	2.834E-02	2.355E-03	7.496E+01	7.099E+01
5	2.500E+02	1.176E+01	9.770E-01	-1.596E+02	-1.635E+02
6	3.000E+02	4.838E-02	4.021E-03	-5.820E+01	-6.216E+01
7	3.500E+02	1.148E+01	9.544E-01	2.844E+01	2.447E+01
8	4.000E+02	3.320E-02	2.759E-03	1.657E+02	1.617E+02
9	4.500E+02	2.450E-02	2.036E-03	1.122E+02	1.082E+02
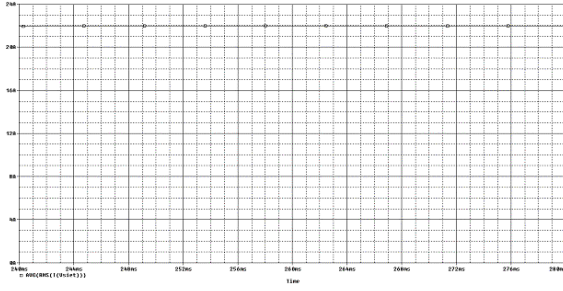
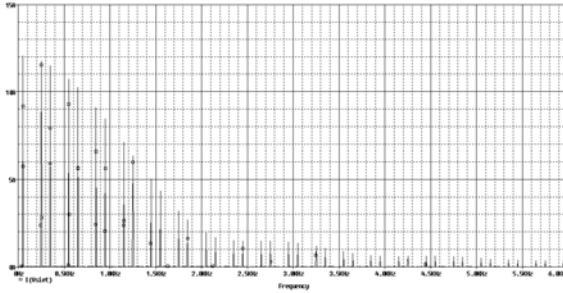**Fig. 45** The RMS value of the phase rectifier current

Fig. 46 The Frequency spectrum of the input phase current

Based on the obtained values, the first harmonic distortion factor of the voltage and the current can now be calculated.

$$k_{dU} = \frac{U_1}{U} = \frac{230}{230} = 1 \tag{57}$$

$$k_{dI} = \frac{I_1}{I} = \frac{12,03}{21,95} = 0,548 \tag{58}$$

Similarly, the total harmonic factor of the voltage and the current can be calculated, too.

$$k_{sU} = \sqrt{\frac{U_2^2 + U_3^2 + ... + U_n^2}{U_1^2 + U_2^2 + U_3^2 + ... + U_n^2}} = \sqrt{\frac{0}{52900}} = 0 \tag{59}$$

$$k_{sI} = \sqrt{\frac{I_2^2 + I_3^2 + ... + I_n^2}{I_1^2 + I_2^2 + I_3^2 + ... + I_n^2}} = \sqrt{\frac{337,0816}{481,8025}} = 0,8364 \tag{60}$$

The amount of the rectifier's active power is:

$$P = 3(U_0 I_0 + \sum_{k=1}^{\infty} \frac{U_{mk} I_{mk}}{2} \cos\varphi_k) = 3.U_1.I_1.\cos\varphi_1 = 3.230.12,03.$$
$$.\cos(3,965^o) = 8280,83 \ \text{W} \tag{61}$$

The rectifier's reactive power is:

$$Q = 3(\sum_{k=1}^{\infty} U_k I_k \sin\varphi_k) = 3.U_1 I_1 \sin\varphi_1 =$$
$$= 3.230.12,03.\sin(3,965^o) = 573,97 \ \text{VAr} \tag{62}$$

The quantity of the apparent power is:

$$S = 3.UI = 3.230.21,95 = 15145,5 \ \text{VA} \tag{63}$$

The distortion power has the value:

$$P_d = \sqrt{S^2 - P^2 - Q^2} = \sqrt{(15145,5)^2 - (8280,83)^2 - (573,97)^2} =$$
$$= 12668,25 \ \text{VAd} \tag{64}$$

Figure Fig. 47 displays the comparison of the one phase and three-phase bridge rectifier net currents during its one half-period. The one phase rectifier has only one current impulse, the amplitude and duration of which are bigger as in the case of three phase rectifier currents. Even though its RMS values are almost the same.
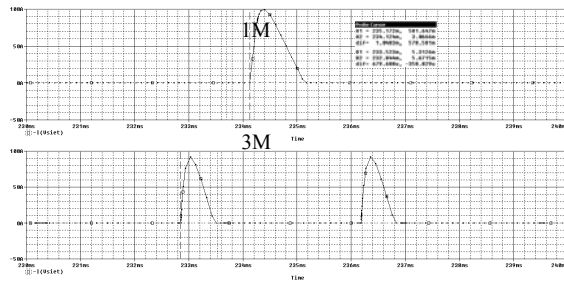

Fig. 47 The currents comparison of the both rectifiers during its one half-period

On the basis of the performed analyses, it is evident, that even though the first harmonic distortion factors and total harmonic factors are the same in both cases, so the three-phase rectifier provides three times higher output power. However, it especially provides more smoothed output of the DC voltage and a thinner spectrum of higher harmonics in the input current, because all multiples of the 3rd harmonic frequencies are eliminated. So more effective filtering of higher harmonics is enabled. In both cases, the direct rectifier connection to the feeding net without utilizing of the filters is undesirable, due to too big contents of the phase current higher harmonics.

3. CONCLUSION

The performed analysis enables to the electrical equipment constructers to improve the EMC parameters of the newly constructed devices not only by expensive testing measurements, but also in advance, by the theoretical analysis and simulation. They can state its supposed and required properties by a predictive method based on the results introduced in this paper. The improving of EMC will thus be more comfortable, cheaper, easier and quicker.

REFERENCES

[1] Kováč, D. - Kováčová, I.: The influence of Utilizing Static Power Semiconductor Converters on Quality of Electrical Power Line Parameters, Quality Innovation Prosperity, 2001, No. 1, pp. 74-84

[2] Šimko, V. - Kováčová, I.: The transient actions in impulse converters with DC voltage feeding circuit, Theoretical Electrical Engineering at Technical Universities, West Bohemian University Plzeň, No. 4, 1994, pp. 91-96

[3] Kaňuch, J.: Investigation methodology design of the EMC for drives with disc motor, Dissertation thesis, FEI TU Košice, 2005.

[4] Pálka R.: Elektrical machines IV – design of DC machines, Publishing center SVŠT in Bratislava, 1983.

[5] Servalco Servomotors, firm catalogue of Axem.

[6] Kotal M., Novotný P., Voženílek P.: Calculation examples of rotation electrical machines, Publishing center ČVUT in Prague, 1988.

BIOGRAPHIES

Kováčová Irena - She finished her studies in 1982 at the Technical University of Košice, Department of Electrical Drives, area - Power electronics with excellent evaluation. From this time she has worked at the Department of Electrical Drives, first as an assistant lecturer and now as an associate professor. In 1988 she got her doctoral diploma. In 1991 she got the Award of the Minister of Education for the Development of Science and Technology. Her working interest is mainly focused on the field of power electronics, especially on the construction of converters and inverters with new perspective elements and computer simulation of new power semiconductor parts and devices.

Ján Kaňuch - He finished his studies in 1986 at the Technical University of Košice, Department of Electrical Drives and area – Electrical machines. From this time he has worked at the Department of Electrical Drives as an assistant lecturer. His working interest is mainly focused on the field of construction of electrical machines, electrical equipments for motor-cars and electrical apparatuses.

Kováč Dobroslav - He finished his studies in 1985 at the Technical University of Košice, Department of Electrical Drives, area - Power electronics with excellent evaluation. Then he worked as a research worker at the Department of Electrical Drives. His research work was focused on the practical application of new power semiconductor devices. In 1989 he got the Award of the Minister of Education for the Development of Science and Technology. From 1991 he has worked as assistant lecturer at the Department of Theoretical Electrical Engineering and Electrical Measurement. He got his doctoral diploma in 1992 for the work on the field of power electronics. From 2000 he has worked as professor and his working interest is now focused mainly on the field of computer simulation of power electronic circuits and automated computer measuring.